Evaluating the Stability of Outang Landslide in the Three Gorges Reservoir Area Considering the Mechanical Behavior With Large Deformation of the Slip Zone

Junbiao Yan
China University of Geosciences
Zongxing Zou (zouzongxing@cug.edu.cn)
China University of Geosciences https://orcid.org/0000-0002-5660-5864
Rui Mu
China University of Geosciences
Xinli Hu
China University of Geosciences
Jincheng Zhang
Chongqing Geological Disaster Prevention Center
Wen Zhang
Chongqing Geological Disaster Prevention Center
Aijun Su
China University of Geosciences
Jinge Wang
China University of Geosciences
Tao Luo
China University of Geosciences

Research Article

Keywords: Landslide evolution, Slip zone soil, Repeated direct shear test, Constitutive model, Shear mechanical behavior, Large deformation

Posted Date: January 18th, 2022

DOI: https://doi.org/10.21203/rs.3.rs-819772/v1

Version of Record: A version of this preprint was published at Natural Hazards on February 21st, 2022.
See the published version at https://doi.org/10.1007/s11069-022-05276-0.

Evaluating the stability of Outang landslide in the Three Gorges Reservoir area considering the mechanical behavior with large deformation of the slip zone

Junbiao Yan[a, b, e], Zongxing Zou[a, b*], Rui Mu[a, b], Xinli Hu[c], Jincheng Zhang[d], Wen Zhang[d], Aijun Su[a, b], Jinge Wang[a, b], Tao Luo[a, b]

[a] (Badong National Observation and Research Station of Geohazards, China University of Geosciences, Wuhan, 430074, China)

[b] (Three Gorges Research Center for Geo-hazards, China University of Geosciences, Wuhan, 430074, China)

[c] (School of Engineering, China University of Geosciences, Wuhan, 430074, China)

[d] (Chongqing Geological Disaster Prevention Center, Chongqing, 401147, China)

[e] (State Key Laboratory of Geomechanics and Geotechnical Engineering, Institute of Rock and Soil Mechanics, Chinese Academy of Sciences, Wuhan, 430071, China)

[*] Corresponding author.

E-mail address:

yanjunbiao@cug.edu.cn (J. Yan); zouzongxing@cug.edu.cn (Z. Zou); murui@cug.edu.cn (R. Mu); huxinli@cug.edu.cn (X. Hu); 88659503@qq.com (J. Zhang); 54233312@qq.com (W. Zhang); aijunsu@cug.edu.cn (A. Su); wangjinge@cug.edu.cn (J. Wang); 18296760919luotao@cug.edu.cn (T. Luo)

Abstract

The large deformation mechanical properties of slip zone soil play an important role in the stability evolution of landslide. The traditional landslide stability evaluation method can only be used to calculate a single stability factor, which cannot dynamically evaluate the landslide stability as it evolves. The large deformation mechanical properties of slip zone soil from Outang landslide in the Three Gorges Reservoir area are investigated by the indoor repeated direct shear test. Based on the damage theory, the shear damage behavior of slip zone soil with large shear displacement is analyzed, and a mechanical model describing the relationship between shear stress and shear displacement in accordance with the mechanical mechanism of landslide is established. Then, the stability of Outang landslide is dynamically evaluated by skillfully combining the mechanical model and the residual thrust method. The results show that the slip zone soil has obvious softening behavior and constant residual strength under the condition of large deformation. The model with clear physical meaning can reflect the large displacement shear mechanical properties of slip zone soil, which is consistent with the test results. The stability factor of Outang landslide gradually decreases and tends to be constant as landslide moves. The mechanical mechanism of the landslide stability evolving with deformation is the strain softening behavior of the slip zone soil, and the mechanical mechanism of the landslide stability evolving with water level is the reduction of effective stress in anti-sliding section under the influence of reservoir water. It is suggested that active measures should be taken in time in the prevention and control of landslide, and the construction of drainage engineering should be paid attention to for large-scale bank landslides.

Keywords: Landslide evolution; Slip zone soil; Repeated direct shear test; Constitutive model; Shear mechanical behavior; Large deformation

1 Introduction

The reservoir landslide is a common geological hazard in the reservoir area, and its instability has a serious impact on the operation of the reservoir area and the safety of ship navigation (Zhang et al. 2021a, b; Wang and Zhang 2021). Since the first impoundment of the Three Gorges Project in 2003, a large number of landslides in the reservoir area have revived. According to statistics, there are 4256 landslides on the bank from Yichang to Jiangjin in the Three Gorges Reservoir area (Tang et al. 2019), such as the Outang landslide that directly threatened the safety of more than 4,000 residents in Anping Town (Luo and Huang 2020), the Huangtupo landslide that caused the relocation of Badong County (Tang et al. 2015a; Juang 2021) and the Qianjiangping landslide that made more than 1,000 people homeless (Jian et al. 2014). Large shear deformation of slip zone usually occurs in the process of reservoir landslide evolution (Zhang et al. 2020; Hu et al. 2021; Li et al. 2021), and affects the landslide stability (Kimura et al. 2014; Yin et al. 2016).

The large shear deformation of slip zone soil is a continuous deforming process. Ring shear test is often used to study the shear mechanical behavior of slip zone soil with large displacement (Chen et al 2021; Sassa et al. 2014; Riaz et al. 2019; Vithana et al. 2012). However, the limited ring shear test can only be used to determine the shear mechanical properties of slip zone soil under the limited normal stress level, and the shear mechanical properties of slip zone soil based on the test level cannot be directly incorporated into the stability evolution analysis of landslide. Traditionally, the peak strength (Jian et al. 2009; Zhang et al. 2013; Loi et al. 2017; Tu et al. 2019) or residual strength (Yu et al. 2018; Ghahramani and Evans 2018) of slip zone soil is used in landslide stability analysis, which only considers the local shear mechanical behavior of the slip zone soil. However, the shear stress in the slip zone soil evolves with large shear deformation (Li et al. 2013; Vadivel and Sennimalai 2019; Stark and Hussain 2010; Kimura et al. 2014). Therefore, the stability of landslide evolves

gradually with deformation (Sun et al. 2015; Tang et al. 2015b; Tang et al. 2017), and dynamically evaluation of the landslide stability is required.

Exploring the relationship between stress and deformation of slip zone soil and establishing the corresponding constitutive model is the prerequisite for landslide stability analysis (Su et al. 2021). Currently, many ideal plastic constitutive models are applied to numerical simulation, such as Mohr-Coulomb ideal plastic constitutive model (Dawson et al. 1999; Griffiths and Lane 1999; Wei and Cheng 2010) and Drucker-Prager ideal plastic constitutive model (An et al. 2019). Obviously, these models ignore the post peak deformation behavior of the soil. Therefore, many strain softening constitutive models have been proposed to consider the softening behavior of the soil (Lo and Lee 1973; Chai and Carter 2009; Yuan et al. 2020; Chen et al. 1992). However, these strain softening models are simplified, which cannot well reflect the actual softening behavior of the soil. In fact, the landslide has large displacement shear deformation along the slip zone (Tan et al. 2018), the mechanical model that can describe the relationship between shear strength and shear displacement can more directly reflect the dynamic mechanical behavior of the landslide. Therefore, it is of great theoretical and practical significance to study the large displacement shear mechanical properties of slip zone soil and establish a shear constitutive model that can reflect the large displacement shear mechanical behavior of slip zone soil.

In this study, the Outang landslide in the Three Gorges Reservoir area is taken as an example. The large displacement shear mechanical behavior of slip zone soil from Outang landslide is studied by indoor repeated direct shear test firstly. Based on the test results, the damage theory is introduced to analyze the shear damage behavior of the slip zone soil, and corresponding shear constitutive model is established. Finally, the evolution characteristics of Outang landslide are investigated by combining the shear constitutive model and residual thrust method, and the mechanical mechanism

of the evolution of the Outang landslide is analyzed.

2 Materials and tests

2.1 Materials

The Outang landslide is located in Anping Town, Fengjie County, Chongqing City (Fig. 1 (a)), on the South Bank of the Yangtze River (Fig. 1 (b)). The landslide is 1990 m long in the North-South longitudinal direction and 899 m wide in the East-West transverse direction, with a total area of 1.769 million m^2 and an overall volume of 89.5 million m^3. It is a typical large deep bedding bedrock landslide in the Three Gorges Reservoir area (Fig. 1 (c) and (d)) (Luo and Huang 2020; Wang et al. 2021). From the Yangtze River to the mountain, the Outang landslide is composed of Slide 1, Slide 2 and Slide 3 (Fig. 1 (c) and (d)). The front elevation of the landslide is 90 ~ 102 m, and the rear elevation of the landslide is 705 m.

The slip zone soil used in the test was taken from the 1# drainage tunnel (Fig. 1 (c)), where the slip zone of the Slide 1 is revealed (Fig. 1 (d)). The slip zone soil is mainly the argillization product of carbonaceous claystone and carbonaceous shale, which is black and gray black, with high clay content, luster and good toughness. The natural density of the slip zone soil is 2.037 g/cm^3, the natural moisture content is 19.9 %, and the specific gravity of the soil particles is 2.73. The liquid limit and plastic limit of the slip zone soil are 36.3(%) and 16.8(%), respectively. The plastic index I_P is 19.5 and the liquid index I_L is 0.16. The soil is hard plastic clay.

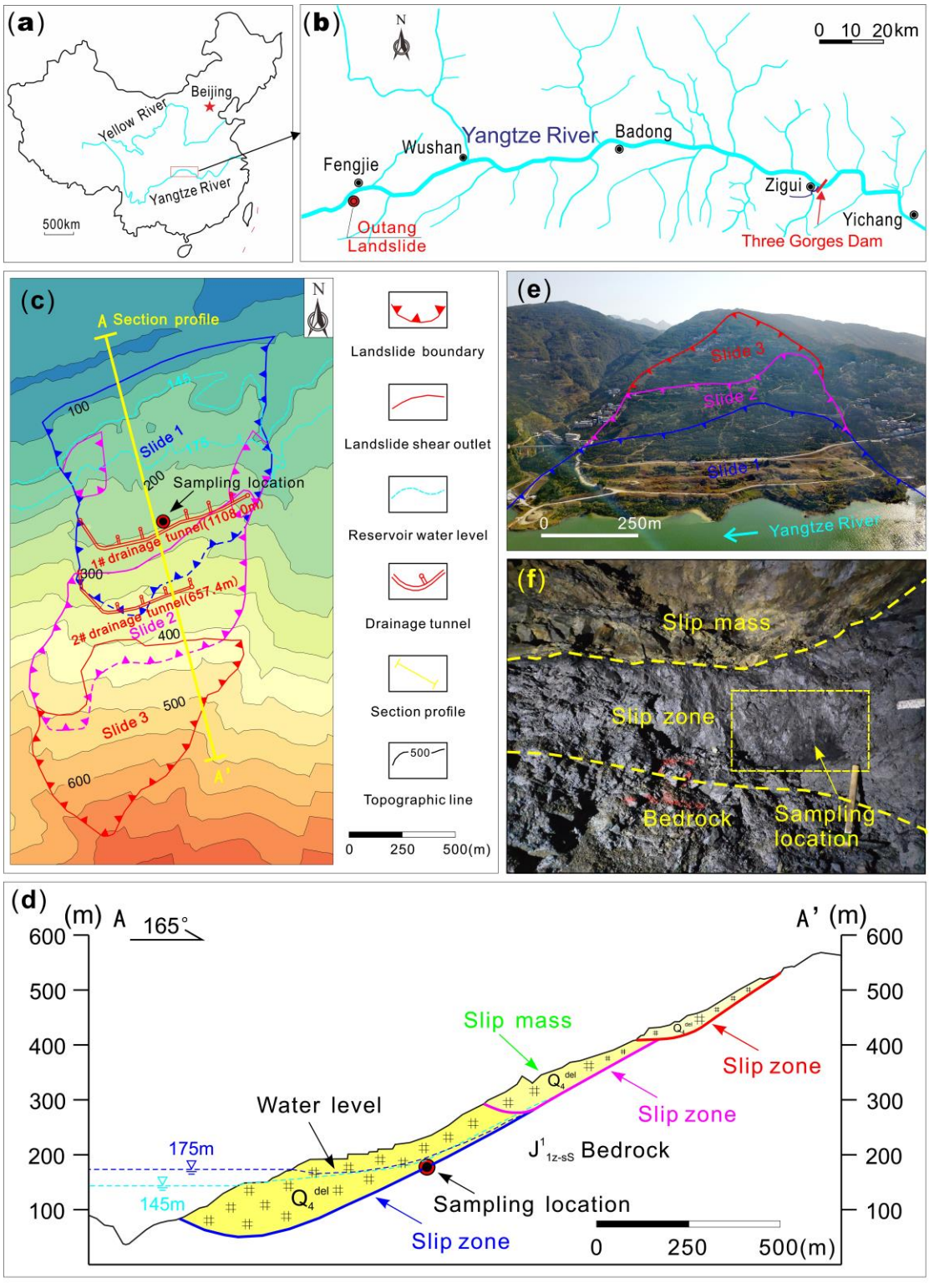

Fig. 1. Comprehensive geological map of Outang landslide. (a) and (b) are the geographical location of the landslide; (c) is plain view of the landslide; (d) is the main section of the landslide; (e) shows the overall view of the landslide; (f) shows the slip zone of the landslide (exposed in 1# drainage tunnel).

2.2 Repeated direct shear tests

Landslides often undergo large shear deformation, and the simple direct shear test commonly used in engineering can only achieve the shear displacement of about 10-12 mm. Although direct shear test can be used to determine the pre peak stage and part of the post peak stage in the shear deformation process of slip zone soil, it cannot be used to determine the residual strength of slip zone soil. The repeated direct shear test is developed based on the simple direct shear test. When the simple direct shear test is finished, it does not stop the test, but carries on the reverse shear to realize the repeated shear of the soil in turn (Chen and Liu 2014; Wen and Jiang 2017). The maximum shear displacement of each shear is 10-12mm. Theoretically, the infinite shear displacement can be achieved by repeated direct shear test. Generally, the residual strength of cohesive soil can be achieved only by repeated shearing for 3-4 times.

In order to obtain the whole shear deformation process of the slip zone soil, repeated direct shear tests were carried out by using strain controlled direct shear apparatus. Considering the in-situ geological conditions of the soil, the dry density and moisture content of the soil samples were controlled to be consistent with the undisturbed soil, that is, the remolded soil samples with dry density of 1.70g/cm^3 and moisture content of 19.9% were prepared for repeated direct shear tests. The normal consolidation stress is set to 800kPa. After the consolidation is stable, the normal stress required for the test is set, and then the shear begins. The transmission device pushes the lower shear box at a constant rate to form a shear plane in the soil. In the first forward shear test, the shear displacement range of the direct shear apparatus should be reached to obtain the complete strain softening stage as far as possible. In the later shear tests, only for the purpose of obtaining the residual strength. When the shear stress changes little, the specimen can be pushed back for the next forward shear. Generally, the clay sample is repeatedly sheared for 3-4 times, and when the residual stress is basically constant, it can be considered that the slip zone soil has reached the

residual state, and the shear strength in this state is the residual strength of the slip zone soil. Each group of repeated direct shear test should not be less than four soil samples, that is, four different normal stresses should be set. The repeated direct shear test scheme is listed in Table 1.

Table 1 Scheme of repeated direct shear test for the slip zone soil of Outang landslide

Number	Consolidation stress / (kPa)	Normal stress / (kPa)
RDS-1	800	100
RDS-2	800	200
RDS-3	800	300
RDS-4	800	400

The relationship between shear stress and shear displacement of the slip zone soil obtained from repeated direct shear test (τ-u curve) is shown in Fig. 2. After three times of repeated shear for each sample, the residual shear stress of the slip zone soil is basically constant. It can be considered that the slip zone soil has basically reached the residual strength state by the third shear. When the specimen is pushed back reversely, the specimen is also in the state of being sheared, but the direct shear test apparatus has no reverse force measuring device. In order to obtain the complete shear deformation and failure process curve, the missing reverse shear process can be approximately connected by spline curve based on the existing test data points (Fig. 2). Due to the main purpose of the last two shear tests is to obtain the residual strength of the slip zone soil, and the test results also show that the residual strength is almost constant, and the pre peak stage and part of the post peak stage of the τ-u curve have been completely controlled by the first forward shear test. Therefore, it is reasonable to obtain the whole shear deformation and failure process of the slip zone soil by repeated direct shear test.

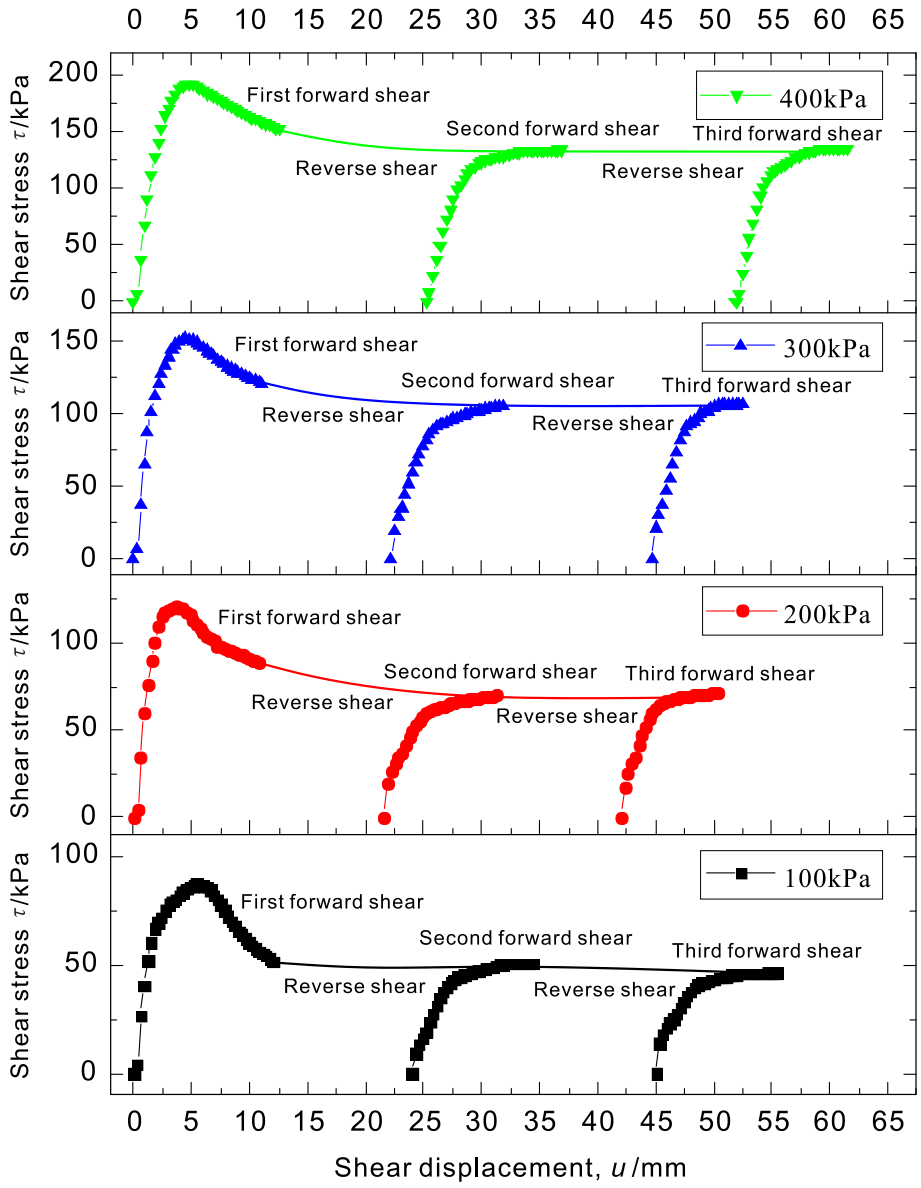

Fig. 2. Shear stress - shear displacement curve in repeated direct shear test

As shown in Fig. 2, in the first forward shear test (which can be regarded as conventional direct shear test), the shear strength of the soil gradually increases with shear deformation, but the increase rate of shear strength gradually slows down. After the shear stress reaches the peak value, the shear stress significantly decreases, and the decrease rate also gradually slows down. The soil shows obvious strain softening phenomenon. In addition, the slip zone soil has greater shear strength under the condition of high normal stress, but the shear stress decays more slowly in the process of strain softening. It shows that the strain softening phenomenon is less obvious under the condition of higher normal stress, which indicates that the strain softening

phenomenon is closely related to the over consolidation ratio of the soil, and the degree of strain softening decreases with the decrease of over consolidation ratio. In the last two shear tests, the shear strength of the soil decreased significantly due to the formation of shear plane. At the same time, the growth rate of the initial shear stress (the slope of the initial section of the curve) is also smaller than that of the first shear. In addition, the soil does not show the phenomenon of strain softening, and the shear stress in the soil remains constant or slightly increases under large displacement, which shows the phenomenon of strain hardening. The shear stress - shear displacement curves of the last two shears are basically the same, and tend to a stable residual strength. The slight strain hardening of the soil during the last two shear processes is mainly due to the macro shear surface has been generated in the soil, the cohesion in the soil has been basically lost, and the shear strength of the soil is mainly the friction strength, which is essentially the bite or sliding action between soil particles. After the shear surface is formed, the friction strength is basically unchanged, so the shear strength of the soil remains basically constant or slightly hardened as the deformation increases, rather than obvious strain softening like the first forward shear.

Due to the reversal of the shear direction, the unloading process inevitably occurs in the repeated direct shear test. Usually, the unloading process will restore the elastic deformation. However, the landslide has large deformation, so the slip zone soil also has large displacement shear process. The elastic deformation in the large displacement shear process is so slight that it can be ignored compared with the total deformation. In addition, we mainly focus on the shear strength of the slip zone soil. After large displacement deformation, the slip zone soil basically reaches the residual strength stage, and the residual strength does not evolve with the deformation. Therefore, we believe that the unloading process does not affect our test results in the repeated direct shear test.

According to the shear test results, no matter what kind of normal stress

conditions, the slip zone soil shows the same deformation and failure trend in the process of large displacement shear, which can be divided into five typical stages (Fig. 3).

(1) Pore shear compaction stage (**oa** section): during the initial deformation of the soil, the pores in the shear zone are compacted along the direction of shear stress under the action of shear stress. Compared with the elastic deformation stage, the soil has relatively large displacement deformation under smaller shear stress. The shear deformation caused by pore compaction in the soil is slight, so this section will be ignored in the later analysis.

(2) Linear elastic deformation stage (**ab** section): the shear stress increases linearly with the shear displacement, and the slope of the straight line is defined as the shear stiffness K_s, which is a physical value describing the elastic shear deformation of the soil. There is no plastic deformation and damage in this stage.

(3) Plastic hardening stage (**bc** section): the starting point **b** in this stage is the yield point, which means that the soil will undergo plastic deformation after this point. The corresponding shear displacement at this point is defined as shear yield displacement u_y. The growth rate of shear stress in this stage gradually decreases.

(4) Strain softening stage (**cd** section): the shear stress decreases significantly after point **c**, and the soil presents obvious strain softening phenomenon. The shear stress at point **c** reaches the maximum and the maximum shear stress is defined as the peak strength τ_p. The decrease of shear strength in this stage is mainly due to the formation of shear plane in the shear process, which leads to the decrease of the soil cohesion. At the same time, the directional arrangement of the soil particles also leads to the decrease of internal friction angle.

(5) Residual strength stage (**de** section): the soil is in the failure stage, and the shear stress in the soil is basically constant, which is named residual shear strength τ_r.

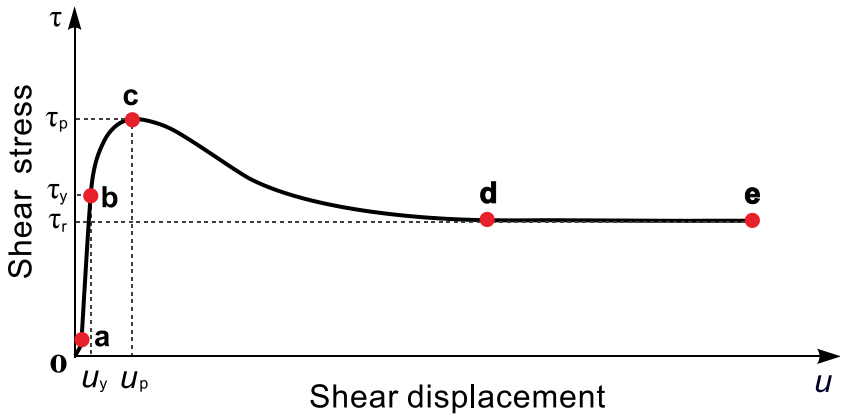

Fig. 3. Whole shear deformation and failure process of the slip zone soil (Zou et al. 2020)

3 Model

3.1 Shear damage analysis of the slip zone soil

The evolution process of soil strength can be analyzed from the perspective of micro damage. In the process of the soil being sheared, the plastic deformation of the soil leads to micro damage of the soil structure, and the mechanism of plastic deformation is the loss of cementation in the soil and the directional arrangement of the soil particles, so the shear strength of the soil evolves with deformation. In fact, the slip zone soil also has the same shear damage process in the real landslide, which can be confirmed by the extrusion and wrinkling phenomenon of the slip zone and the mirror phenomenon of the slip zone soil observed in the field (Fig. 1(f)). According to the damage theory, the soil can be divided into many micro elements with the same size. Each micro element is composed of undamaged part (or intact part) and damaged part (Fig. 4). With the development of shear deformation of the soil, the undamaged part is transformed into the damaged part, and the damaged part cannot be transformed into the undamaged part due to irreversible plastic deformation. The stress analysis of a representative micro element in the shear state (Fig. 4) shows that the load in the micro element is jointly borne by the intact part and the damaged part (Yang et al. 2015). According to the static equilibrium condition in the *x* direction, the following equation holds:

$$\tau l = \tau' l_1 + \tau'' l_2 \tag{1}$$

where τ represents the shear stress in the micro element; τ' is the shear stress in the intact part, τ'' is the shear stress in the damaged part; l is the section length of the micro element; l_1 and l_2 are the section length of the undamaged part and the damaged part of the micro element, respectively, $l = l_1 + l_2$.

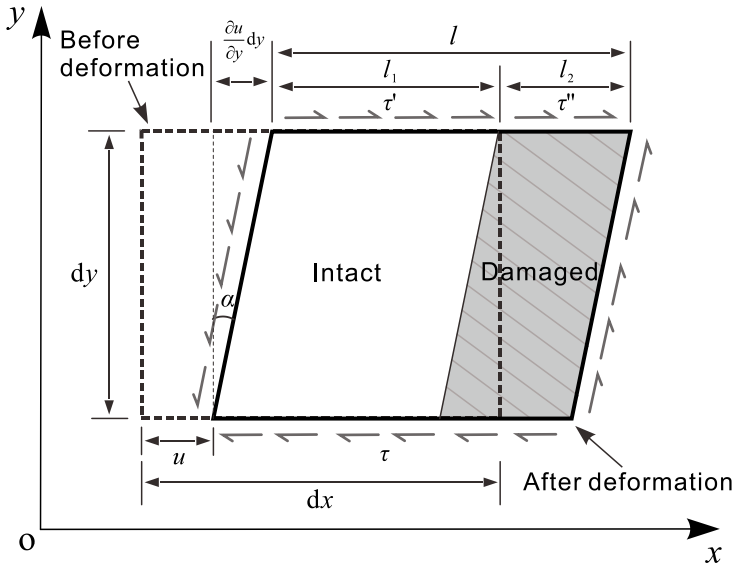

Fig. 4. Representative micro element damage mechanics model of the slip zone soil during shear

The damage degree can be considered as the ratio of the cross-sectional area of the damaged part (l_2dy in Fig. 4) to the total cross-sectional area of the micro element (ldy in Fig. 4) (Hamdi et al. 2011), i.e. $D = \frac{l_2}{l}$, which can be regarded as the proportion of the damaged part in the soil in physical meaning. Divide both sides of Eq. (1) by l to obtain:

$$\tau = \tau(1 - D) + \tau'' D \tag{2}$$

The physical meaning of Eq. (2) is the evolution process of shear stress in the slip zone soil during shear deformation and failure. The damage degree D is a physical value reflecting the evolution process, which varies with the shear deformation of the soil, ranging from 0 to 1.

3.2 Establishment of the model

According to the above shear damage analysis, the shear strength of the undamaged part and the damaged part can be obtained from the shear test results. The undamaged part of the slip zone soil obeys linear elastic deformation, and Hooke's law is applicable. Therefore, the shear strength of the undamaged part is as follows:

$$\tau'=G\gamma \tag{3}$$

where G is the shear modulus, γ is the shear strain.

According to the elastic theory, the shear strain can be expressed by geometric equation:

$$\gamma=\frac{\partial u}{\partial y}+\frac{\partial v}{\partial x} \tag{4}$$

where u and v are the displacements in x direction (shear direction) and y direction (normal direction) of the slip zone soil during shear deformation and failure, respectively (Fig. 4).

In real landslide or shear test, the normal compression v is tiny compared with the landslide displacement or shear displacement u in the shear test, so the shear strain component $\frac{\partial v}{\partial x}$ caused by the normal displacement v can be neglected compared with the shear strain component $\frac{\partial u}{\partial y}$ caused by the shear displacement u. Therefore, the shear strain Eq. (4) can be simplified as

$$\gamma=\frac{\partial u}{\partial y} \tag{5}$$

Substituting Eq. (5) into Eq. (3), the following equation can be obtained:

$$\tau'=G\frac{\partial u}{\partial y} \tag{6}$$

Integrating Eq. (6) from 0 to h along the $\boldsymbol{y}$ direction and noting that the partial derivative $\frac{\partial u}{\partial y}$ can be written as the full derivative $\frac{\mathrm{d}u}{\mathrm{d}y}$, the following equation holds:

$$\int_0^h \tau' dy = Gu \tag{7}$$

where h is the effective shear thickness of the slip zone or the shear zone in the shear test.

From Eq. (7), it follows that

$$\tau' h = Gu \tag{8}$$

Let $K_s = \frac{G}{h}$. Then, Eq. (8) can be simplified as

$$\tau' = K_s u \tag{9}$$

Define K_s as the shear stiffness with a unit of kPa/mm. K_s is the slope of the linear elastic deformation stage in Fig. 3.

In the residual strength stage, all intact elements in the slip zone soil have been transformed into damage elements, so the shear stress in the damaged part is the residual strength τ_r (Fig. 3):

$$\tau'' = \tau_r \tag{10}$$

Substituting Eq. (9) and Eq. (10) into Eq. (2) to obtain:

$$\tau = K_s u(1 - D) + \tau_r D \tag{11}$$

From Eq. (11), the damage degree directly reflects the evolution of shear stress in the slip zone soil. The damage degree can be solved from the perspective of statistical damage theory. It is assumed that the micro element strength of the slip zone soil obeys Weibull probability distribution (Weibull 1951; Krajcinovic and Silva 1982) in the process of shear damage (Lai et al. 2012):

$$p(x) = \frac{m}{u_0}\left(\frac{x}{u_0}\right)^{m-1} \exp\left[-\left(\frac{x}{u_0}\right)^m\right] \tag{12}$$

where m is the shape parameter and u_0 is the scale parameter. The meaning of the two parameters will be discussed in detail later.

Assuming that the micro elements of the slip zone soil have the same size, the overall shear damage process of the slip zone soil is analyzed, and the overall damage degree is determined by the proportion of the number of damaged elements N_D to the

total number of elements N:

$$D = \frac{N_{\mathrm{D}}}{N} \tag{13}$$

The micro element strength level of the slip zone soil reflects the risk degree of shear deformation and failure (Zou et al. 2020). With the shear process of the slip zone soil, the distribution variable x increases from 0 to U, and the damage micro element N_{D} is expressed as follows:

$$N_{\mathrm{D}} = N\int_0^U \{\frac{m}{u_0}(\frac{x}{u_0})^{m-1}\exp[-(\frac{x}{u_0})^m]\}dx = N\{1-\exp[-(\frac{U}{u_0})^m]\} \tag{14}$$

The damage degree is determined by combining Eq. (13) and Eq. (14):

$$D = 1-\exp[-(\frac{U}{u_0})^m] \tag{15}$$

where U is the distribution variable reflecting the risk degree of shear deformation of the slip zone soil. The shear displacement of the slip zone soil is the macroscopic reflection of its micro damage. In addition, whether in the shear test and landslide displacement monitoring, the shear displacement, as a parameter to intuitively describe the shear deformation of the slip zone soil, can be easily obtained from the shear test and landslide displacement monitoring. Therefore, the shear displacement u is selected as the distribution variable to represent the damage of the slip zone soil.

When the shear deformation of the slip zone soil is before the yield point, that is, $u < u_{\mathrm{y}}$, only elastic deformation occurs in the soil, and the damage degree is equal to zero. The damage only occurs in the soil when the shear deformation exceeds the yield point. Therefore, according to Eq. (15), the damage degree D based on shear deformation is as follows:

$$D = \begin{cases} 0, (u < u_{\mathrm{y}}) \\ 1-\exp[-(\dfrac{u-u_{\mathrm{y}}}{u_0})^m], (u \geq u_{\mathrm{y}}) \end{cases} \tag{16}$$

Eq. (16) is the damage evolution equation of the slip zone soil, which describes the cumulative growth process of damage degree with the increase of shear

deformation. By substituting Eq. (16) into Eq. (11), the shear stress evolution equation of the slip zone soil is obtained as follows (Zou et al. 2020):

$$\tau = \begin{cases} K_s u, (u < u_y) \\ K_s u \left\{ \exp[-(\frac{u-u_y}{u_0})^m] \right\} + \tau_r \left\{ 1 - \exp[-(\frac{u-u_y}{u_0})^m] \right\}, (u \geq u_y) \end{cases} \tag{17}$$

where the parameters K_s, u_y and τ_r can be obtained by shear stress - shear displacement curve. The parameters u_0 and m in the model can also be further determined based on the properties of the curve.

3.3 Solution of parameters

The model parameters u_0 and m can be solved by adopting the property of peak point of τ - u curve in the shear test. The strength corresponding to the peak point is often used in engineering practice, and it is often considered that the soil begins to fail after the deformation reaches the peak point in the shear test. Therefore, the peak point of the curve is of great practical significance, and it is more reasonable to use the properties of the peak point to determine the model parameters u_0 and m. It is considered that the model curve and test data reach the same peak point, and the following equation holds:

$$\left. \frac{\partial \tau}{\partial u} \right|_{u=u_p} = 0, \ \tau|_{u=u_p} = \tau_p \tag{18}$$

where u_p and τ_p are the shear displacement and shear stress corresponding to the peak point of the τ - u curve, respectively (Fig. 3).

Substituting Eq. (11) into Eq. (18) produces the following equation:

$$\begin{cases} \left. \frac{\partial \tau}{\partial u} \right|_{u=u_p} = \left[K_s(1-D) + (\tau_r - K_s u) \frac{\partial D}{\partial u} \right]_{u=u_p} = 0 \\ \tau_p = K_s u_p (1 - D|_{u=u_p}) + \tau_r D|_{u=u_p} \end{cases} \tag{19}$$

From Eq. (16), the following equation is obtained:

$$\frac{\partial D}{\partial u} = \frac{m}{u_0} (\frac{u-u_y}{u_0})^{m-1} \exp[-(\frac{u-u_y}{u_0})^m], (u \geq u_y) \tag{20}$$

In combination with Eq. (16), Eq. (19) and Eq. (20), the parameters u_0 and m can

be calculated as follows:

$$m = \frac{K_s(u_p - u_y)}{(K_s u_p - \tau_r)\ln(\frac{K_s u_p - \tau_r}{\tau_p - \tau_r})}, \quad u_0 = \frac{u_p - u_y}{\sqrt[m]{\ln(\frac{K_s u_p - \tau_r}{\tau_p - \tau_r})}} \tag{21}$$

where all parameters can be obtained by the shear test.

3.4 Model validation

According to the shear test results, the model test parameters were calculated. The pore shear compaction stage is ignored. The slope of the τ - u curve in the linear deformation stage is the shear stiffness K_s, the end of the linear deformation stage is the yield point, the displacement corresponding to the yield point is the yield displacement u_y, and the displacement and stress at the peak point of the curve are determined as the peak displacement u_p and peak strength τ_p, the constant shear strength during the third shear is the residual strength τ_r. It should be noted that the repeated direct shear test is only to determine the residual strength of the slip zone soil, and other test parameters are obtained from the first forward shear test. Therefore, some data points in the whole process of deformation and failure that cannot be fully captured in the repeated direct shear test have no effect on the determination of parameters. The distribution parameters m and u_0 are calculated by Eq. (21). According to Fig. 2, the calculation results of all parameters are listed in Table 2.

Table 2 Model parameters of slip zone soil of Outang landslide

normal stress σ_n (kPa)	shear stiffness K_s (kPa/mm)	yield displacement u_y (mm)	peak displacement u_p (mm)	Peak strength τ_p (kPa)	residual strength τ_r (kPa)	u_0 (mm)	m
100	43.787	1.5	5.4	87.0903	46.3243	1.8711	0.5842
200	61.182	1.8	3.6	120.843	71.4201	1.5566	0.6712
300	63.001	2.1	4.5	152.0955	106.3974	1.4826	0.6302
400	68.678	2.4	5.1	191.8842	135.2886	1.7276	0.6463

The model curve can be obtained by substituting the calculated parameters (Table 2) into Eq. (17). In addition, the repeated direct shear test results are compared with the model curve, as shown in Fig. 5.

As shown in Fig. 5, the model curve has the same deformation and failure trend as the test results, showing typical shear mechanical behavior consistent with the whole deformation and failure process, and the method of calculating Weibull parameters m and u_0 based on peak point control has a clear physical meaning, so that the model curve completely consistent with the test data at the peak point. In addition, the damage evolution Eq. (16) used in the model is a 'S' type growth equation. Under large shear displacement, the damage degree evolves to 1, and the shear strength of the soil reaches a constant residual strength, which can be well shown in the comparison between the model curve and the test data, that is, the model curve and the test data reach the same residual strength. It should be noted that in the repeated direct shear test, the purpose of the latter two shear tests is only to achieve large displacement shear to obtain the residual strength stage of the soil, and the pre peak stage and partial strain softening stage of the τ-u curve are completely controlled by the first direct shear test. By comparing the model curve with the first direct shear test data and the residual strength stage test data, it can be seen that the model has good properties, especially under high normal stress (200kPa, 300kPa and 400kPa), the model curve is in good agreement with the test results. Under the condition of low normal stress (100kPa), due to the large overconsolidation ratio of the slip zone soil, its properties are more brittle, and the strain softening phenomenon is obvious, which leads to a large deviation between the model curve and the test data in the strain softening stage. However, the Outang landslide is a large-scale deep landslide, and the normal stress in the geological environment where the slip zone is located is basically high stress. Therefore, the model is reliable in the evaluation of the stability evolution of the Outang landslide, which will be discussed in detail in the following chapters.

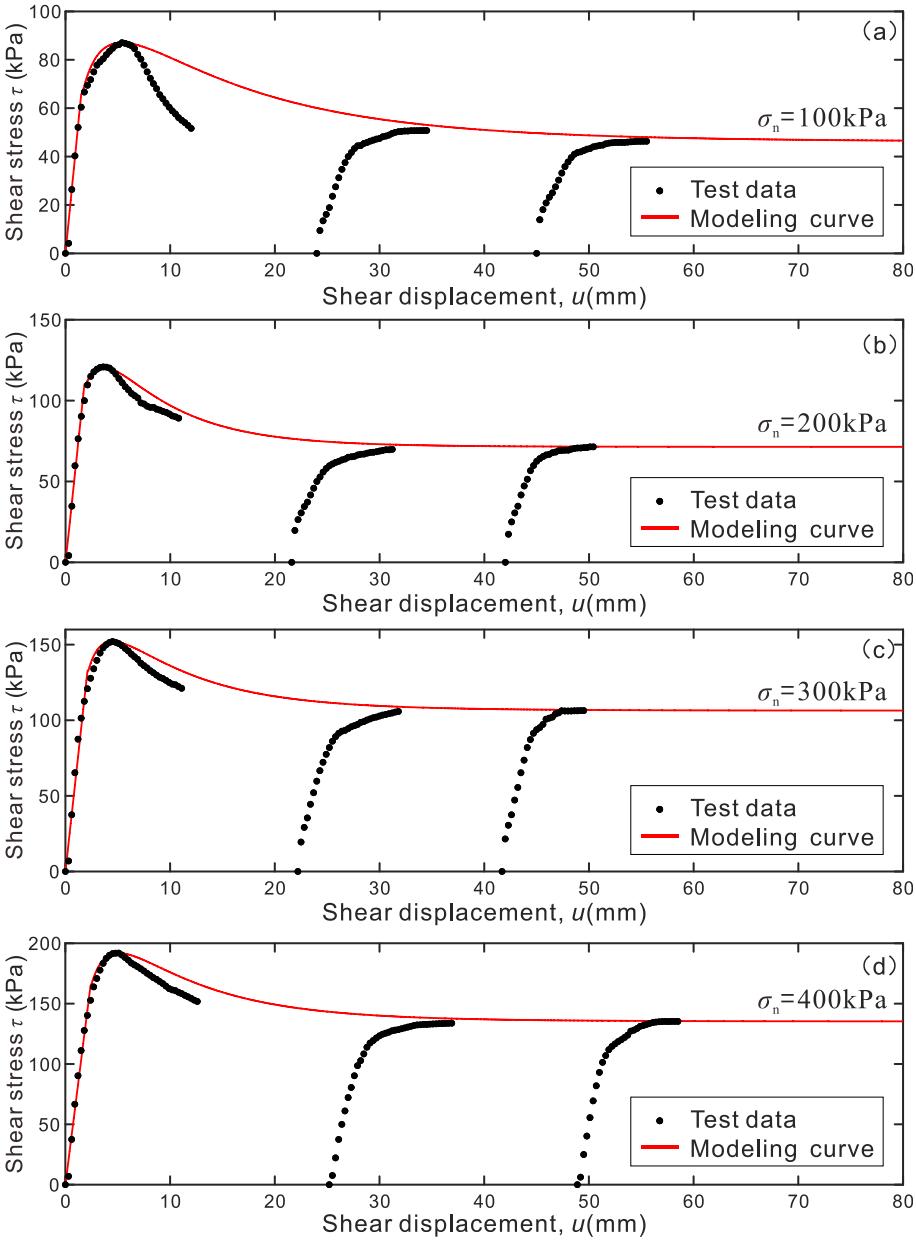

Fig. 5. Comparison of model curves and shear test results

3.5 Parameter study

3.5.1 Shear test parameters

In the shear test, the shear mechanical behavior of the slip zone soil is different under different normal stresses, that is, the shear test parameters are only related to the normal stress (Table 2). The relationship between shear test parameters and normal stress is analyzed, and the relationship is linearly fitted with reference to the classical Coulomb formula (Fig. 6). Under the condition of low normal stress (100kPa), the peak displacement and normal stress deviate from the linear correlation, while the

linear correlation between peak displacement and normal stress is obvious under high normal stress. Generally, the normal stress plays a role in resisting the shear deformation, so as the normal stress increases, the soil is less prone to damage, that is, the displacement required to reach the peak stress is greater. In addition, the geological environment of the slip zone soil of the Outang landslide is in a state of high stress. Therefore, when studying the more general law between the peak displacement and the normal stress, only the data points under the higher normal stress (200KPa, 300kPa and 400kPa) are used for fitting analysis.

Fig. 6 shows that the shear stiffness K_s is approximately positively correlated with the normal stress, and the mechanical mechanism of positive correlation between shear stiffness and normal stress is mainly the friction between the soil particles. The relationship between yield displacement u_y, peak displacement u_p and normal stress is also linear positive correlation. Similarly, the mechanism of this positive correlation is also the restraining effect of normal stress on the shear deformation of the soil. The normal stress restrains the shear deformation of the soil macroscopically and the micro damage of the soil microscopically, so that the shear displacement required for the soil to reach the yield or failure state is larger. The relationship between shear strength and normal stress is the classical Coulomb formula. As shown in Fig. 6 (d), both peak shear strength and residual shear strength have good linear positive correlation with normal stress, and the corresponding shear strength parameters are as follows: peak cohesion c_p=51.569kPa, peak internal friction angle φ_p=19.07°, residual cohesion c_r=14.389kPa, residual internal friction angle φ_r=16.80°. The decrease of shear strength parameter is due to the gradual accumulation of damage in the slip zone soil with the formation of shear plane in the large displacement shear process.

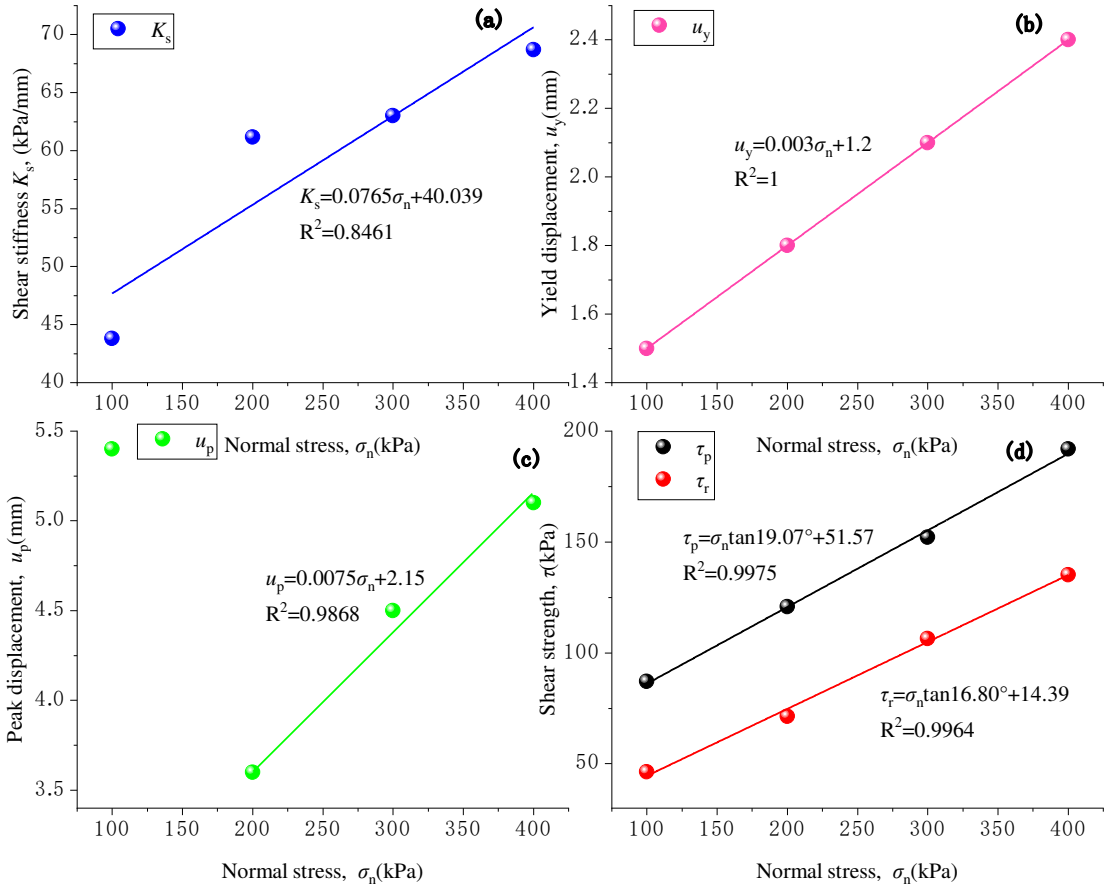

Fig. 6. Parameter analysis of shear stress - shear displacement curve. (a) shear stiffness K_s, (b) yield displacement u_y, (c) peak displacement u_p, (d) shear strength τ

3.5.2 Model parameters of Weibull distribution

The model test parameters including shear stiffness, yield displacement, peak displacement and shear strength have clear physical meanings and directly reflect the shear mechanical properties of the soil. For Weibull distribution parameters m and u_0, the control variable method can be used to study their unique physical meaning. Taking the 200 kPa model curve as an example, other parameters except m remain unchanged. A series of model curves with different m values are obtained by using the model in this paper, as shown in Fig. 7. Fig. 7 shows that the parameter m has a significant effect on the strain softening behavior of the soil. As m increases, the slip zone soil has a faster attenuation rate from the peak stress to the residual stress, the strain softening phenomenon is more obvious, and the soil shows more obvious brittleness. In order to quantify the strain softening degree of the soil in the process of

strain softening, the slope of the model curve can be calculated. The slope of the τ-u curve in the strain softening stage reflects the attenuation rate of the shear strength of the soil. Since the shear strength of the soil in the softening stage gradually decays, the slope of the curve should be negative. Considering the softening stage, the derivation of the first equation of Eq. (17) is obtained:

$$\frac{d\tau}{du}=K_s u\left\{\exp[-(\frac{u-u_y}{u_0})^m]\right\}+(K_s u-\tau_r)\left\{-\frac{m}{u_0}(\frac{u-u_y}{u_0})^{m-1}\exp[-(\frac{u-u_y}{u_0})^m]\right\},(u\geq u_y) \tag{22}$$

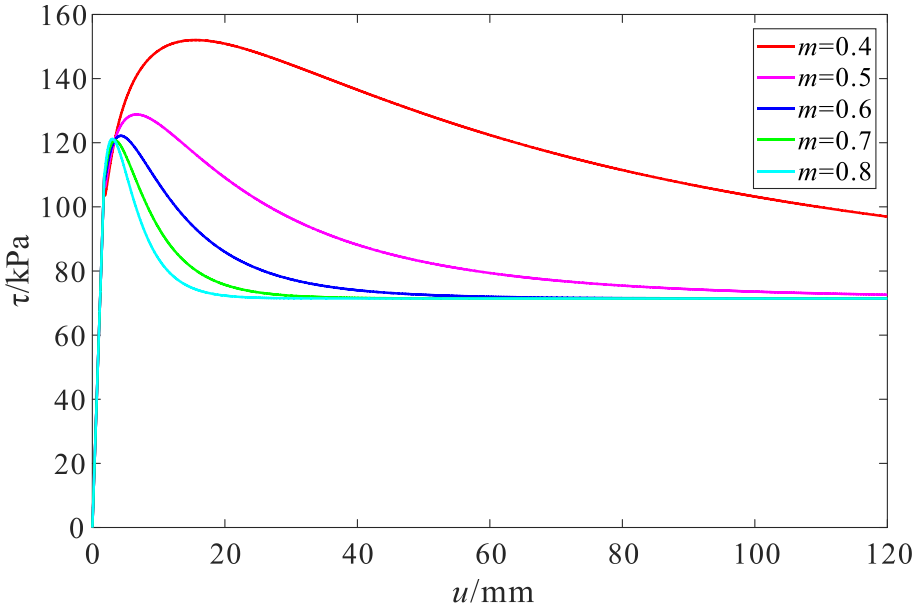

Fig. 7. Model curves under various m

According to Eq. (22), the slope of the curve in Fig. 7 is shown in Fig. 8 (a). The part of the curve less than 0 in Fig. 8 (a) corresponds to the strain softening stage in Fig. 7. Obviously, the larger the m is, the larger the absolute value of the slope in the strain softening stage is, indicating that the faster the shear stress decay rate is, and the more brittle the soil is. Furthermore, the absolute value of the extreme value of the slope dτ/du of the softening stage curve reflects the extreme value of the strength decay rate of the soil, which can represent the equivalent of the strength decay rate of the soil, so the new brittle index I_B of the slip zone soil is defined:

$$I_B=\left|\frac{d\tau}{du}\right|_{\max}=\left|\frac{d\tau}{du}\right|_{\frac{d^2\tau}{du^2}=0},(\frac{d\tau}{du}<0) \tag{23}$$

According to Eq. (23), the brittleness index I_B under different m is calculated, and the relationship between I_B and m is plotted (Fig. 8 (b)). According to Fig. 8 (b), the brittleness index I_B increases with the increase of m, and shows an obvious parabola correlation, which fully shows that the parameter m is a physical value influencing the strain softening degree or brittleness index of the slip zone soil in terms of shear mechanical properties.

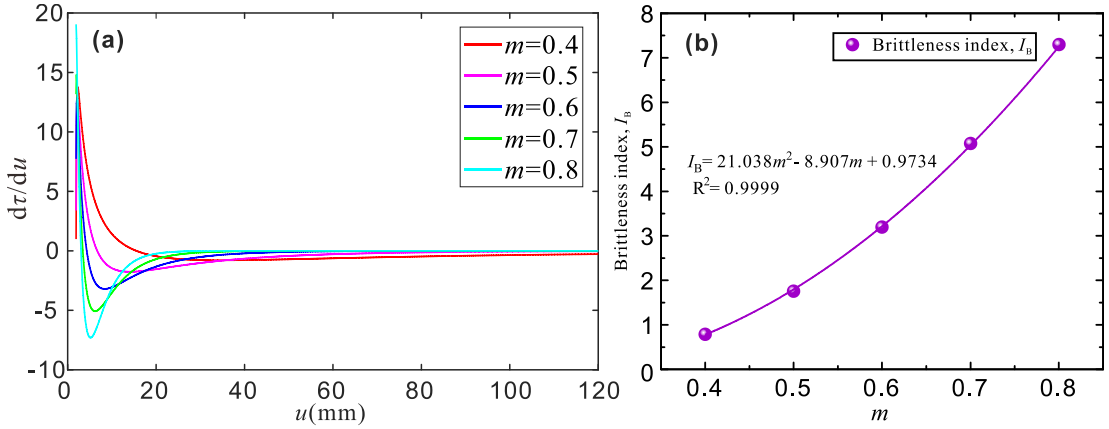

Fig. 8. Brittle analysis of the slip zone soil. (a) the slope dτ/du curve under various m (b) relationship between I_B and m

In addition, considering the stability of the landslide, since the stability of the landslide is directly related to the shear strength of the slip zone soil, the attenuation of the shear strength of the slip zone soil is also closely related to the attenuation of the landslide stability. If the slip zone soil has a large brittleness index, the stability of the landslide will decay faster, and this kind of landslide is a sudden landslide. On the contrary, if the slip zone soil has a small brittleness index, the stability of the landslide will decline more slowly, and this kind of landslide is a creep landslide. Therefore, on the level of landslide evolution, m is a physical value that affects the evolution rate of the landslide stability.

Similarly, in order to analyze the role of parameter u_0 in the model, a series of τ-u curves under various u_0 are shown in Fig. 9. Fig. 9 shows that the peak strength and peak displacement of the model curve increase with parameter u_0, while the residual strength tends to converge to a constant value. Different from the effect of parameter m, the shear strength decay rate of the model curve in the strain softening

stage is basically the same under different u_0. The parameter u_0 mainly affects the peak displacement and peak strength. Quantitatively, the relationship between peak displacement, peak strength and u_0 is plotted in Fig. 10. Fig. 10 shows that with the increase of u_0, the peak displacement and peak strength of the slip zone soil show an increasing trend. Therefore, it can be concluded that u_0 is a physical value reflecting the peak displacement and peak strength.

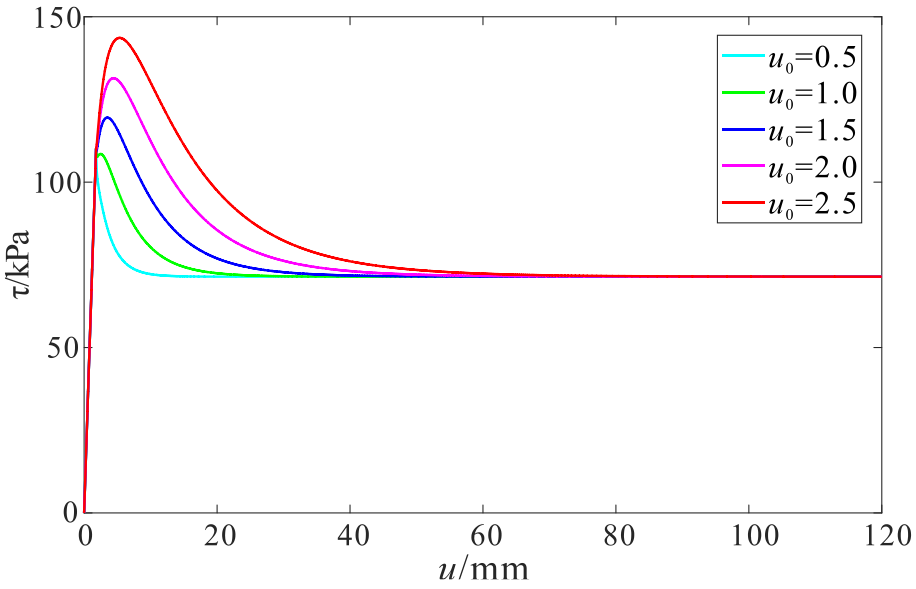

Fig. 9. Model curve under various u_0

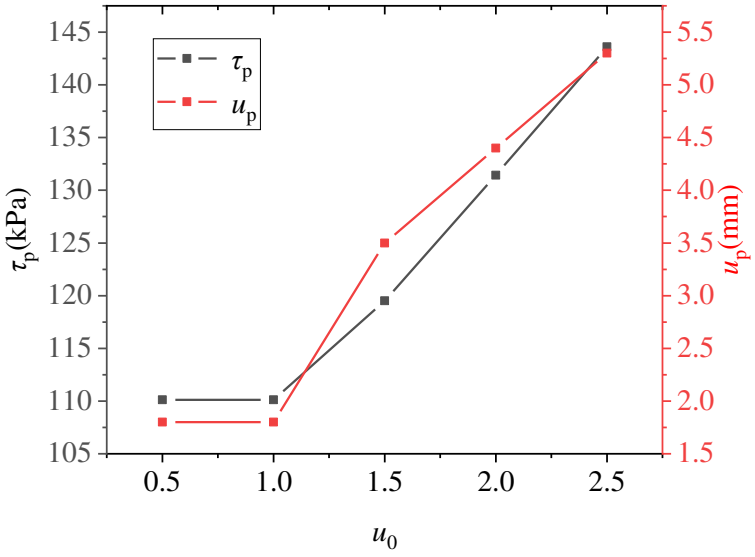

Fig. 10. Relationship between peak strength, peak displacement and u_0

4 Applications

4.1 Dynamic evaluation method of landslide stability

Generally, the peak strength or residual strength of slip zone soil is used to calculate a single stability factor to evaluate the stability of landslide. Therefore, the traditional landslide stability analysis method fails to consider the strain softening behavior of the slip zone soil, and it cannot be used to study the evolution process of landslide with deformation. The shear constitutive model that fully considers the large displacement shear mechanical behavior of slip zone soil can be used to evaluate the stability evolution of landslide. Since the sliding surface of Outang landslide is not a regular arc shape, but a multi-level and multi-segment broken line shape, the residual thrust method can be well applied to the stability analysis of the landslide with a broken line sliding surface (Zhang and Zhang 2008). Therefore, the shear constitutive model is combined with the residual thrust method to realize the dynamic evaluation of Outang landslide stability considering the large displacement shear deformation.

The shear strength of the slip zone soil evolves with the displacement, which leads to the stability factor of landslide evolves with the displacement. The typical main section of Outang landslide (Fig. 1(d)) is selected as the calculation section. According to the force balance condition of the landslide slice along the sliding surface direction (Fig. 11), the residual thrust P_i of slice i based on the strength reduction method is as follows:

$$P_i = P_{i-1}\cos(\alpha_{i-1} - \alpha_i) + T_i - R_i / F_{\mathrm{r}} \tag{24}$$

where $P_{i\text{-}1}$ represents the residual thrust of slice i-1; $\alpha_{i\text{-}1}$ and α_i are the inclination angles of the sliding surface at slice i-1 and slice i, respectively, and the inclination angle of the sliding surface at the anti - warping part of the landslide is negative; T_i represents the sliding component of the gravity of the slice i, $T_i=W_i\sin\alpha_i$; W_i is the gravity of slice i, and the soil and water are analyzed as a whole. When the sliding force is calculated under the condition of stable seepage field, the saturated gravity

549 should be used; When the landslide is submerged below the reservoir water level,
550 there is no stable seepage field below the groundwater level, and the effective gravity
551 should be used for the gravity of the soil below the water level when calculating the
552 sliding force, that is, W_i=W_{1i}+W_{2i}, W_{1i} is the gravity of the part of slice i above the
553 groundwater level, W_{2i} is the gravity of the part of slice i below the groundwater level
554 (calculated by saturation gravity or effective gravity based on whether a stable
555 seepage field exists or not); R_i is the anti - sliding force of slice i (Fig. 11); F_r is the
556 overall strength reduction factor.

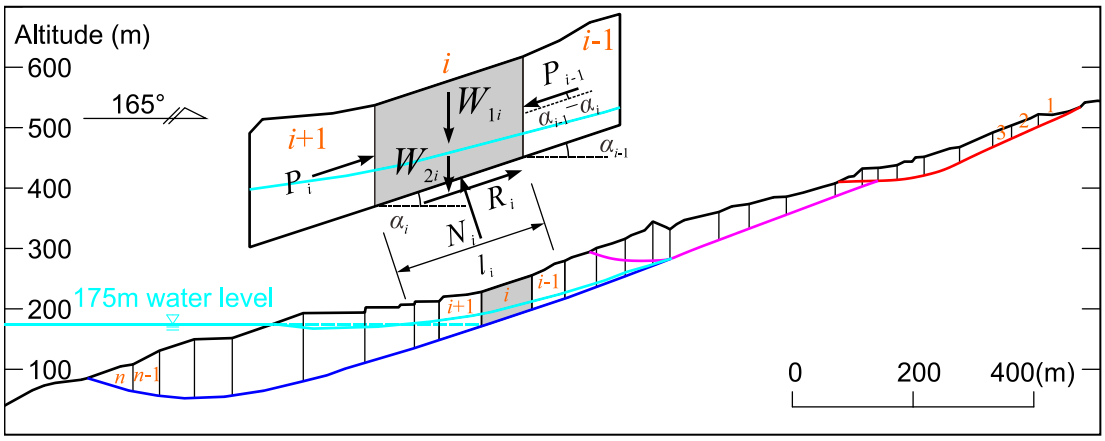

557

558 Fig.11. Force analysis of the slices of Outang landslide

559 The anti - sliding force R_i of the slice i in Eq. (24) can be calculated by the shear
560 strength:

561 $$R_i = \tau_i l_i \tag{25}$$

562 where τ_i represents the shear strength provided by the slip zone at the slice i, which is
563 related to the normal stress σ_{ni} and shear displacement u, and can be calculated by the
564 shear constitutive model; l_i represents the length of the slip zone at the slice i (Fig.
565 11).

566 Considering the effect of the thrust P_i transferred from the previous slice, the
567 effective normal force N_i on the slip zone at the slice i is as follows:

568 $$N_i = P_{i\text{-}1}\sin(\alpha_{i-1} - \alpha_i) + W_i'\cos\alpha_i \tag{26}$$

569 where W_i' is the effective gravity of slice i, W_i'=W_{1i}+W_{2i}', and W_{2i}' is the effective
570 gravity of the part of slice i below the groundwater level, that is, the effective gravity

of the soil below the water level is used to calculate the anti - sliding force regardless of whether there is stable seepage field or not.

Thus, the normal stress σ_{ni} on the slip zone at the slice i is obtained according to Eq. (26):

$$\sigma_{ni} = \frac{P_{i\text{-}1}\sin(\alpha_{i-1} - \alpha_i) + W_i{}'\cos\alpha_i}{l_i} \tag{27}$$

Under the condition of the preset strength reduction factor F_r, the residual thrust is calculated one by one from the first slice at the rear edge of the landslide by Eq. (24), and the residual thrust P_n of the slice n at the front edge of the landslide can be obtained. When the residual thrust P_n is equal to 0, the landslide is in a critical state between stability and instability, which is called limit equilibrium state. According to the strength reduction method, the strength reduction factor F_r in this state is defined as the stability factor F_s of the landslide.

Since the Eq. (24) for solving the residual thrust contains the shear strength τ_i, and the equation of the shear strength τ_i is the shear constitutive model (Eq. (17)), which is an exponential function. In the shear constitutive model, all parameters are only related to the normal stress σ_{ni}, so the evolution of shear strength τ_i with displacement u is only related to the normal stress σ_{ni}, and each landslide slice has different normal stress. Therefore, the solution of landslide stability factor is a highly nonlinear problem, and the analytical expression of stability factor cannot be obtained, which can be calculated by iterative method. The detailed flow of landslide dynamic stability evaluation method is shown in Fig. 12.

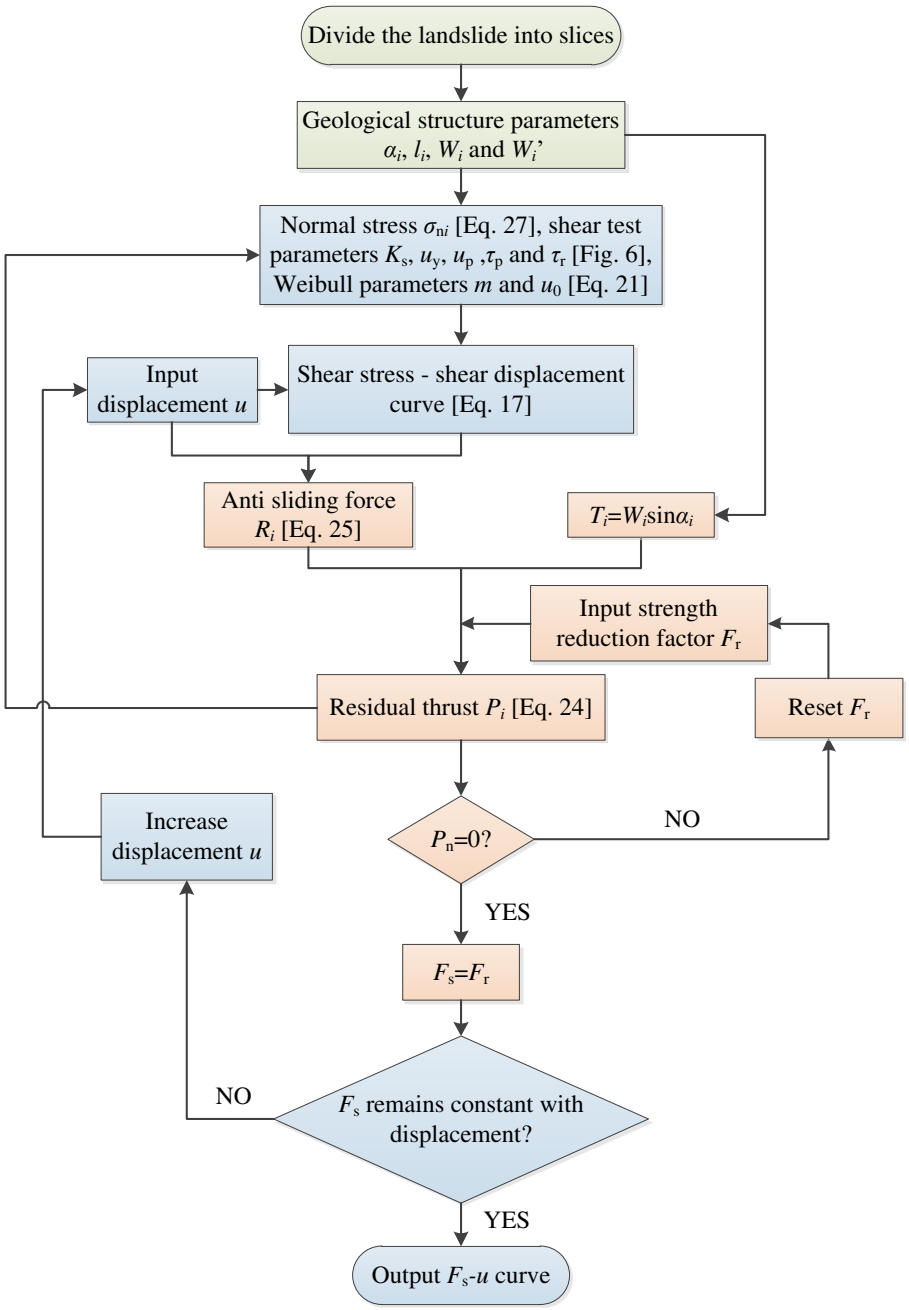

592

593 Fig.12. Flow of landslide dynamic stability evaluation method

594 Different from the traditional limit equilibrium method based on strength
595 parameters, cohesion c and internal friction angle φ, the landslide dynamic stability
596 evaluation method in this paper is realized by calculating the shear stress evolution
597 curve with known normal stress and combining with the residual thrust method, rather
598 than directly using cohesion c and internal friction angle φ to calculate the landslide
599 stability. The advantage of this method is that the strength parameters are implicitly
600 included in the model, and the evolution of the shear strength of the slip zone with

displacement is also fully considered.

4.2 Stability evolution characteristics of Outang landslide

In order to study the effect of reservoir water level on the stability of Outang landslide and provide theoretical guidance for the drainage engineering of Outang landslide, the stability evolution of Outang landslide without considering groundwater condition and 175m water level condition is analyzed respectively. Since the pre peak stage of the τ-u curve of the slip zone soil has little reference significance, and the maximum peak displacement is predicted to be about 17 mm within the range of the maximum normal stress (2000 kPa) where the slip zone of Outang landslide is located, so the evolution law of the landslide stability with the displacement after the displacement reaches 17 mm is studied (Fig. 13). Fig. 13 shows that with the increase of landslide displacement, the landslide stability factor decreases at a gradually decreasing attenuation rate, and the stability factor tends to a constant value under large displacement, which is consistent with the strain softening phenomenon of the slip zone soil: the shear strength gradually decreases with displacement and tends to be constant until reaching the residual strength stage. Fig. 13 shows that the displacement required for a constant stability factor is greater than the displacement required for the slip zone soil to reach the residual strength stage. This reason is that the Outang landslide is a deep giant landslide, and the normal stress at the location of the slip zone is high stress, up to 2000kPa, the strain softening phenomenon of the slip zone soil is less obvious under large normal stress, and the displacement required to decay from peak strength to residual strength increases.

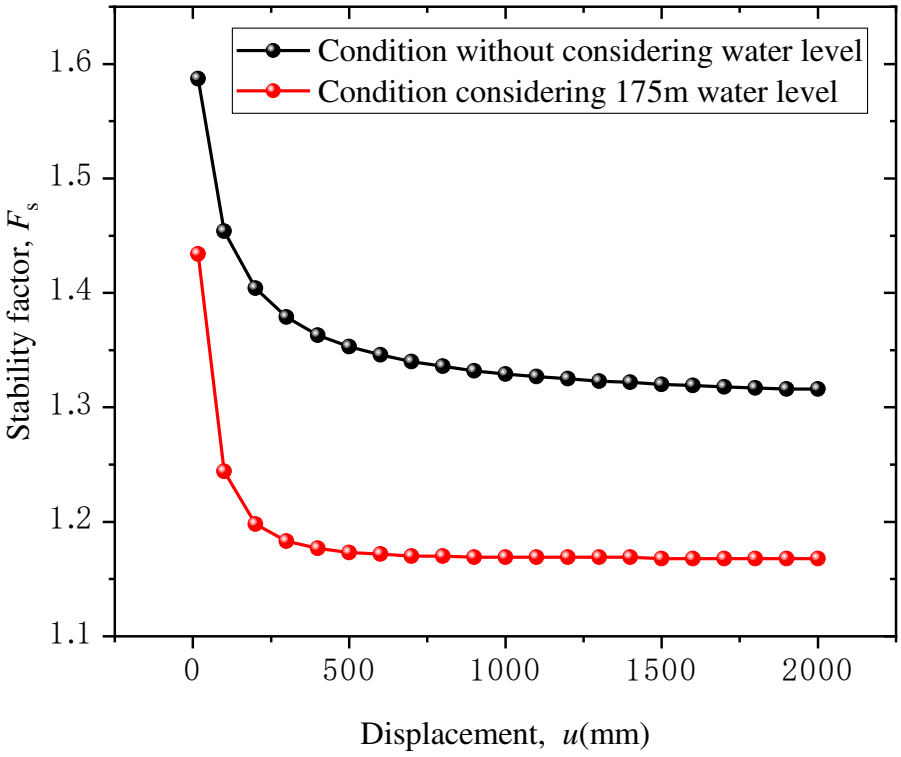

Fig. 13. Stability evolution characteristics of Outang landslide

Without considering the reservoir water level, the stability factor of Outang landslide gradually decreases from 1.587 to 1.316 and remains constant, indicating that the landslide deformation has a significant impact on the stability of the landslide. Therefore, it is suggested that active reinforcement and protection should be implemented in time to prevent the deformation of the landslide, otherwise the gradual reduction of its stability factor leads to more difficult in prevention and control. Under the condition of 175 m reservoir water level, the landslide stability factor gradually evolves from 1.434 to 1.168, and then remains constant. Compared with the condition without considering the water level, the landslide stability factor decays faster, and it only takes about 500 mm displacement for the stability factor to decay to a constant value. From the perspective of mechanical mechanism, the main reason for the faster decline rate of landslide stability is that the reservoir water leads to the decrease of the effective gravity of the front slip mass, the decrease of the gravity of the front slide mass leads to the decrease of the normal stress, and the strain softening phenomenon of the slip zone soil is relatively obvious, resulting in the faster

decline of landslide stability factor.

Comparing the stability of the landslide with or without considering the reservoir water, it is concluded that the reservoir water has a significant impact on the stability of Outang landslide, and the attenuation amplitude of the peak stability factor with the water level $\Delta F_{s\text{-}w}$ is 0.153, and the attenuation amplitude of residual stability factor with the water level $\Delta F_{s\text{-}w}$ is 0.148. The main reason for the effect of reservoir water on landslide stability is that the reservoir water causes the reduction of the effective gravity of the anti-sliding section of the landslide. The front part of the Outang landslide has a small inclination angle and even an inverted section, which is the main anti-sliding section. Affected by the reservoir water, the effective gravity of the anti-sliding section decreases, resulting in the reduction of the effective normal stress and anti-sliding force of the landslide, which leads to the reduction in the landslide stability factor. Therefore, the drainage engineering is a feasible measure for preventing and controlling the large-scale landslide.

5 Conclusion

In this study, the shear mechanical properties of the slip zone soil from Outang landslide under large displacement are studied by repeated direct shear tests. A shear constitutive model of the slip zone soil is established based on damage theory. By combining the residual thrust method, the stability evolution of the Outang landslide without considering the reservoir water and 175m water level is studied. The main conclusions are as follows:

(1) The repeated direct shear test can be well applied to realize the large displacement shear which cannot be realized by the traditional direct shear test, and can well study the residual strength behavior of slip zone soil.

(2) The established shear constitutive model can well reflect the large displacement shear mechanical behavior of the slip zone soil. The parameters in the model have clear physical meaning. The model parameter *m* has a positive parabolic

correlation with the brittleness index, which reflects the strain softening degree of the slip zone soil, and the parameter u_0 has an effect on the peak displacement and peak strength.

(3) The stability factor of Outang landslide gradually decreases and tends to be constant with the deformation of the landslide. The mechanical mechanism of landslide stability evolving with deformation is the strain softening behavior of the slip zone soil. The stability of the landslide under the 175m water level condition is obviously lower than that under the condition without considering the water level, and the stability factor decays faster with the displacement. The mechanical mechanism of the landslide stability evolving with the water level is mainly that the reservoir water affects the effective stress in the anti - sliding section.

(4) It is suggested to strengthen the active prevention and control measures in the landslide prevention and control engineering, and strengthen the construction of drainage engineering for large reservoir bank landslide.

6 Acknowledge

This work was supported by the National Natural Science Foundation of China (Nos. 42020104006, 42077268, 42090055) and the Chongqing Geological Disaster Prevention and Control Center of China (No. 20C0023)

Declaration

Conflicts of interest

The authors declare no conflict of interest.

References

[1] An Y, Wu Q, Shi C, Liu Q (2016) Three-dimensional smoothed-particle hydrodynamics simulation of deformation characteristics in slope failure. Géotechnique 66(8): 670-680.

[2] Chai JC, Carter JP (2009) Simulation of the progressive failure of an embankment on soft soil. Comput Geotech 36(6): 1024-1038.

[3] Chen HE, Ma WL, Yuan XQ, Niu CC; Shi B; Tian GL (2021) Influence of stress conditions on shear behavior of slip zone soil in ring shear test: an experimental study and numerical simulation. Nat Hazards. https://doi.org

/10.1007/s11069-021-05090-0
[4] Chen XP, Liu D (2014) Residual strength of slip zone soils. Landslides 11(2): 305-314.
[5] Chen Z, Morgenstern NR, Chan DH (1992) Progressive failure of the Carsington Dam: a numerical study. Can Geotech J 29(6): 971-988.
[6] Dawson EM, Roth WH, Drescher A (1999) Slope stability analysis by strength reduction. Géotechnique 49(6): 835-840.
[7] Ghahramani N, Evans SG (2018) The 1985 earthquake-triggered North Nahanni rockslide, Northwest Territories, Canada: The co-seismic movement of a sedimentary rock mass conditioned by residual strength. Eng Geol 247: 1-11.
[8] Griffiths DV, Lane PA (1999) Slope stability analysis by finite elements. Géotechnique 49(3): 387-403.
[9] Hamdi E, Romdhane NB, Le Cléac JM (2011) A tensile damage model for rocks: Application to blast induced damage assessment. Comput Geotech 38(2): 133-141.
[10] Hu XL, Wu SS, Zhang GC, Zheng WB, Liu C, He CC, Liu ZX, Guo XY, Zhang H (2021) Landslide displacement prediction using kinematics-based random forests method: A case study in Jinping Reservoir Area, China. Eng Geol 283: 105975.
[11] Jian WX, Wang ZJ, Yin KL (2009) Mechanism of the Anlesi landslide in the Three Gorges Reservoir, China. Eng Geol 108(1-2): 86-95.
[12] Jian WX, Xu Q, Yang HF, Wang FW (2014) Mechanism and failure process of Qianjiangping landslide in the Three Gorges Reservoir, China. Environ Earth Sci 72(8): 2999-3013.
[13] Juang CH (2021) BFTS - Engineering geologists' field station to study reservoir landslides. Eng Geol 284(4):106038.
[14] Kimura S, Nakamura S, Vithana SB, Sakai K (2014) Shearing rate effect on residual strength of landslide soils in the slow rate range. Landslides 11(6): 969-979.
[15] Krajcinovic D, Silva MAG (1982) Statistical aspects of the continuous damage theory. Int J Solids Struct 18(7):551-562.
[16] Lai YM, Li JB, Li QZ (2012) Study on damage statistical constitutive model and stochastic simulation for warm ice-rich frozen silt. Cold Reg Sci Technol 71: 102-110.
[17] Li CD, Criss RE, Fu ZY, Long JJ, Tan QW (2021) Evolution characteristics and displacement forecasting model of landslides with stair-step sliding surface along the Xiangxi River, three Gorges Reservoir region, China. Eng Geol 283: 105961.
[18] Li YR, Wen BP, Aydin A, Ju NP (2013) Ring shear tests on slip zone soils of three giant landslides in the Three Gorges Project area. Eng Geol 154: 106-115.
[19] Lo KY, Lee CF (1973) Stress analysis and slope stability in strain-softening materials. Géotechnique 23(1): 1-11.
[20] Loi DH, Quang LH, Sassa K, Takara K, Dang K, Thanh NK, Van TP (2017) The

28 July 2015 rapid landslide at Ha Long City, Quang Ninh, Vietnam. Landslides 14(3): 1207-1215.
[21] Luo SL, Huang D (2020) Deformation characteristics and reactivation mechanisms of the Outang ancient landslide in the Three Gorges Reservoir, China. B Eng Geol Environ 79(8): 3943-3958.
[22] Riaz S, Wang GH, Basharat M, Takara K (2019) Experimental investigation of a catastrophic landslide in northern Pakistan. Landslides 16(10): 2017-2032.
[23] Sassa K, Dang K, He B, Takara K, Inoue K, Nagai O (2014) A new high-stress undrained ring-shear apparatus and its application to the 1792 Unzen–Mayuyama megaslide in Japan. Landslides 11(5): 827-842.
[24] Stark TD, Hussain M (2010) Shear Strength in Preexisting Landslides. J Geotech Geoenviron 136(7): 957-962.
[25] Su ZY, Wang GZ, Wang YK, Luo X, Zhang H (2021) Numerical simulation of dynamic catastrophe of slope instability in three Gorges reservoir area based on FEM and SPH method. Nat Hazards. https://doi.org/10.1007/s11069-021-05075-z
[26] Sun GH, Zheng H, Tang HM, Dai FC (2016) Huangtupo landslide stability under water level fluctuations of the Three Gorges reservoir. Landslides 13(5): 1167-1179.
[27] Tan QW, Tang HM, Fan L, Xiong CR, Fan ZQ, Zhao M, Li C, Wang DJ, Zou ZX (2018) In situ triaxial creep test for investigating deformational properties of gravelly sliding zone soil: example of the Huangtupo 1# landslide, China. Landslides 15(12): 2499-2508.
[28] Tang HM, Li CD, Hu XL, Su AJ, Wang LQ, Wu YP, Criss RE, Xiong CR, Li Y (2015a) Evolution characteristics of the Huangtupo landslide based on in situ tunneling and monitoring. Landslides 12(3): 511-521.
[29] Tang HM, Wasowski J, Juang CH (2019) Geohazards in the three Gorges Reservoir Area, China – Lessons learned from decades of research. Eng Geol 261: 105267.
[30] Tang HM, Yong R, Ez Eldin MAM (2017) Stability analysis of stratified rock slopes with spatially variable strength parameters: the case of Qianjiangping landslide. B Eng Geol Environ 76(3): 839-853.
[31] Tang HM, Zou ZX, Xiong CR, Wu YP, Hu XX, Wang LQ, Lu S, Criss RE, Li CD (2015b) An evolution model of large consequent bedding rockslides, with particular reference to the Jiweishan rockslide in Southwest China. Eng Geol 186: 17-27.
[32] Tu GX, Huang D, Deng H (2019) Reactivation of a huge ancient landslide by surface water infiltration . J MT SCI-ENGL 16(4): 806-820.
[33] Vadivel S, Sennimalai CS (2019) Failure Mechanism of Long-Runout Landslide Triggered by Heavy Rainfall in Achanakkal, Nilgiris, India. J Geotech Geoenviron 145(9): 04019047.
[34] Vithana SB, Nakamura S, Kimura S, Gibo S (2012) Effects of overconsolidation ratios on the shear strength of remoulded slip surface soils in ring shear. Eng Geol

131-132: 29-36.
[35] Wang JE, Schweizer D, Liu QB, Su AJ, Hu XL, Blum P (2021) Three-dimensional landslide evolution model at the Yangtze River. Eng Geol 292: 106275. https://doi.org/10.1016/j.enggeo.2021.106275.
[36] Wang K, Zhang SJ (2021) Rainfall-induced landslides assessment in the Fengjie County, Three-Gorge reservoir area, China. Nat Hazards. https://doi.org/10.1007/s11069-021-04691-z
[37] Wei WB, Cheng YM (2010) Stability Analysis of Slope with Water Flow by Strength Reduction Method. Soils Found 50(1): 83-92.
[38] Weibull W (1951) A statistical distribution function of wide applicability. ASME J Appl Mech 18: 293-297.
[39] Wen BP, Jiang XZ (2017) Effect of gravel content on creep behavior of clayey soil at residual state: implication for its role in slow-moving landslides. Landslides 14(2): 559-576.
[40] Yang SQ, Xu P, Ranjith PG (2015) Damage model of coal under creep and triaxial compression. Int J Rock Mech Min 80: 337-345.
[41] Yin YP, Xing AG, Wang GH, Feng Z, Li B, Jiang Y (2017) Experimental and numerical investigations of a catastrophic long-runout landslide in Zhenxiong, Yunnan, southwestern China. Landslides 14(2): 649-659.
[42] Yu M, Huang Y, Deng WB, Cheng HL (2018) Forecasting landslide mobility using an SPH model and ring shear strength tests: a case study. Nat Hazard Earth Sys 18(12): 3343-3353.
[43] Yuan WH, Liu K, Zhang W, Dai BB, Wang Y (2020) Dynamic modeling of large deformation slope failure using smoothed particle finite element method. Landslides 17(7): 1591-1603.
[44] Zhang YG, Chen XQ, Liao RP, Wan JL, He ZY, Zhao ZX, Zhang Y, Su ZY (2021a) Research on displacement prediction of step-type landslide under the influence of various environmental factors based on intelligent WCA-ELM in the Three Gorges Reservoir area. Nat Hazards 107: 1709-1729. https://doi.org/10.1007/s11069-021-04655-3
[45] Zhang YG, Tang J, He ZY, Tan JK, Li C (2021b) A novel displacement prediction method using gated recurrent unit model with time series analysis in the Erdaohe landslide. Nat Hazards 105(1): 783-813.
[46] Zhang Y, Xu WY, Shao JF, Zou LF, Sun HK (2013) Comprehensive assessment and global stabilisation measures of a large landslide in hydropower engineering. Eur J Environ Civ En 17(3): 154-175.
[47] Zhang YG, Zhang Z, Xue S, Wang RJ, Xiao M (2020) Stability analysis of a typical landslide mass in the Three Gorges Reservoir under varying reservoir water levels. Environ Earth Sci 79(1). https://doi.org/10.1007/s12665-019-8779-x
[48] Zhang SM, Zhang KC (2008) Probe into landslide stability evaluation. Geotech Eng Tech 22(06):271-276. (in Chinese).
[49] Zou ZX, Yan JB, Tang HM, Wang S, Xiong CR, Hu XL (2020) A shear

822 constitutive model for describing the full process of the deformation and failure
823 of slip zone soil. Eng Geol 276: 105766.